IEEE Access
Multidisciplinary | Rapid Review | Open Access Journal

Date of publication xxxx 00, 0000, date of current version xxxx 00, 0000.

Digital Object Identifier 10.1109/ACCESS.2017.Doi Number

Blue Channel and Fusion for Sandstorm Image Enhancement

YAQIAO CHENG[1], ZHENHONG JIA[1], HUICHENG LAI[1], JIE YANG[2], AND NIKOLA K. KASABOV[3], (Fellow, IEEE)

[1]College of Information Science and Engineering, Xinjiang University, Urumqi 830046, China
[2]Institute of Image Processing and Pattern Recognition, Shanghai Jiao Tong University, Shanghai 200400, China
[3]Knowledge Engineering and Discovery Research Institute, Auckland University of Technology, Auckland 1020, New Zealand

Corresponding author: Zhenhong Jia (jzhh@xju.edu.cn).

This work was supported by the National Science Foundation of China under Grant U1803261 and the International Science and Technology Cooperation Project of the Ministry of Education of the People's Republic of China under Grant DICE 2016–2196.

ABSTRACT Due to the scattering and absorption of light by sandstorm particles, images taken in sandstorm environments have low contrast, color distortion and other degradation problems, which seriously affect outdoor computer vision systems. In this paper, we propose a novel method to enhance images captured in sandstorm weather conditions. First, the method builds on the blending of two images that are directly derived from the original degraded image. Second, we use multilayer decomposition technology to enhance image details and use a blue channel and white balancing technology to restore image contrast and chromaticity. Third, we associate weight maps to improve image edge contrast. Finally, the Laplacian pyramid fusion method is used to obtain the fusion results of the sandstorm-free color correction image. The experimental results demonstrate that the proposed method can effectively restore the fade characteristics of sandstorm-degraded images and improve the clarity of the images. Experimental results via subjective and objective evaluations demonstrate that the proposed method can significantly improve images captured during sandstorm weather conditions, and the results are better than other methods.

INDEX TERMS Blue channel, image fusion, multilayer decomposition, sandstorm-degraded image.

I. INTRODUCTION

In recent years, the occurrence of sandstorm weather has become increasingly frequent, which has seriously affected the quality of our images. This directly affects traffic safety, surveillance systems, and driverless and remote sensing systems. Therefore, the enhancement of sandstorm-degraded images has become an urgent problem that must be addressed. The difference between sandstorm-degraded images and general images is that the visibility of the sandstorm-degraded image is low, which is mainly caused by the scattering and absorption of light by the sandstorm particles during the light propagation process. Absorption reduces light energy, and scattering changes the direction of light propagation, which directly leads to low contrast, color deviation and blur in sandstorm images. Some visibility restoration approaches have been proposed to restore the visibility of degraded images to improve system performance during sandstorm weather conditions. These visibility restoration approaches can be divided into physical model methods and image processing methods.

Based on the atmospheric scattering model, researchers use the dark channel prior (DCP) to restore sandstorm-degraded images by estimating ambient light and transmission [1-4]. Priyadharshini [1] and Wang [2] estimated the transmission by extending the DCP algorithm. Shi [3] proposed a halo-reduced DCP algorithm based on the gray-world theory and an adaptive histogram equalization algorithm. Chen [4] used a combination of mixed spectrum analysis and DCP to repair the color shift. However, due to the scattering and absorption of light by sandstorms, the DCP cannot accurately estimate the transmission, so it cannot restore the sandstorm-degraded image well. To estimate the transmission more accurately, some researchers have used physical models to estimate the thickness of sandstorms [5-11]. Information loss constraints [5] and ambient light differences [6, 7] are used to estimate transmission. Huang [8] proposed a sandstorm thickness

This article has been accepted for publication in a future issue of this journal, but has not been fully edited. Content may change prior to final publication. Citation information: DOI 10.1109/ACCESS.2020.2985869, IEEE Access

estimation model based on Laplacian gamma correction technology to estimate transmission and used white patch Retinex technology to restore the true scene color. To avoid serious artifacts, [9, 10] proposed a depth estimation module, color analysis module and visibility restoration module. Dong [11] proposed the depth development method and depth estimation method based on the two color atmospheric scattering model. Jin [12] and Schechner [13] proposed the image clear adaptive method. Using the geometric framework for analyzing the chromatic effects of atmospheric scattering, [14, 15] studied the geometric constraints of atmospheric conditions on scene color change, the geometric constraints of atmospheric conditions on scene color change were derived, and the scene color was restored by using these constraints. The recovery method based on the Retinex model [16, 17] and Li [16] proposed a new optimization function for regularization conditions of illumination and reflectivity based on the robust Retinex model.

Related research based on image processing has also been carried out, such as algorithms combining spatial and transform domains [18], fusion algorithms [19], and fractional differential theory algorithms [20]. Yang [21] used the red channel as the reference curve to fit the blue and green channel color curves close to the red curve, which converted the sandstorm image into a fog image. Alruwaili [22] proposed a statistically adaptive algorithm. Wang [23] converted the sandstorm-degraded image into CIELAB color space and combined the two chrominance components A and B to complete the color correction and saturation stretching. A fast local Laplacian filter was used to process the luminance component to enhance image details. Tan [24] proposed an automated method that only needed input.

Although some achievements have been made with the current method, the following issues remain. First, because most of the blue light is scattered and absorbed, the DCP or thickness estimation model cannot accurately estimate the sandstorm thickness, which results in the processed image still being covered by the sandstorm. Second, there are still some problems with low contrast, color distortion, and under-/overexposure after image processing.

Therefore, this paper proposes a new method that can improve the contrast and chromaticity of sandstorm-degraded images. Using the advantages of blue channel, multilayer decomposition and multi-scale fusion, this method effectively overcomes the problems of low contrast and insufficient color restoration of sandstorm-degraded images. The following are the key features of our proposed method. First, a blue channel algorithm that uses the atmospheric scattering model to restore the lost contrast by restoring short wavelength-dependent colors is proposed. The blue channel can be interpreted as a variant of the DCP. Second, the image is divided into the base layer and the residual layer using multilayer decomposition technology. Blue channel technology is used to restore the contrast of the sandstorm-degraded image in the base layer, the nonlinear mapping operation is performed to enhance the image details in the residual layer, and the processed base layer and the detail layer are fused. The fused image restores the contrast, and the image details are also enhanced. Third, it is the first time the advantages of multilayer decomposition and multi-scale fusion are combined to restore sandstorm-degraded images. This method can enhance the contrast, chromaticity and edge information of sandstorm-degraded images. It also makes up for the loss of details caused by gamma correction and remedies the inability of white balancing to solve the problem of long-range color casting during multi-scale fusion. Our algorithm are mainly used to deal with the images caused by sandstorms not very strong.

The results of subjective and objective evaluation experiments show that the proposed method can significantly improve the images captured under sandstorm weather conditions, and produce better results than other methods.

II. PROPOSED METHOD

In this section, we propose a novel visibility restoration approach based on a blue channel and fusion strategy to enhance degraded images captured under sandstorm weather conditions. The proposed method consists of four parts: multilayer decomposition, blue channel, white balancing, and multi-scale fusion. First, multilayer decomposition is adopted to enhance the detailed information in the sandstorm-degraded image. Next, a blue channel is utilized to restore short wavelength-dependent colors to restore the degraded image contrast. Then, white balancing is used to restore the fade characteristics of the degraded image. Finally, image fusion is utilized to enhance the edge information and clarity of the degraded image.

A. Multilayer decomposition

For multilayer decomposition, considering that different scale filter operators have different image effects, we treat images processed by various filter operators as image layers with different optical bands. We use the guide filter to filter the initial image. By changing the smoothing scale ε, we can obtain different levels of smooth images. The filtered images and residual images of each layer in the initial image are represented as [25]:

$$O_{\varepsilon_i}(\mathrm{x}) = a_i I(\mathrm{x}) + b_i \tag{1}$$

$$D_i(\mathrm{x}) = O_{\varepsilon_i}(\mathrm{x}) - O_{\varepsilon_{i+1}}(\mathrm{x}) \tag{2}$$

where O is the filtered image, D is the residual image, and a and b are constants.

We select the first filtered image D_1 as the base layer and smooth it with the largest smoothing scale ε_1. Residual images containing gradient information of the scenery require nonlinear mapping operation to enhance image details. We choose the sigmoid function [26] to enhance the residual image. This function can be written as:

This article has been accepted for publication in a future issue of this journal, but has not been fully edited. Content may change prior to final publication. Citation information: DOI 10.1109/ACCESS.2020.2985869, IEEE Access

$$T_i(\mathrm{x})=\begin{cases}\dfrac{t}{1+e^{-s\left(D_i(x)-\bar{D}_i\right)}}+\bar{D}_i-t, -0.5t<D(\mathrm{x})<0.5t\\ D_i(x) \qquad\qquad \text{others}\end{cases} \tag{3}$$

where $T_i(x)$ is the detailed layer, s is the scale parameter, t is the width factor of the nonlinear region, and $\bar{D}_i$ is the mean value of the residual image.

B. Blue channel

Most blue light is scattered and absorbed in sandstorm weather conditions [27, 28], so that images obtained in sandstorm weather conditions show overall yellowing, low contrast and color distortion, which leads to inaccurate DCP estimations of the ambient light and transmission. To solve the above mentioned problems, we propose a blue channel method to restore short wavelength-dependent colors, to recover the sandstorm-degraded image. The image formation model (IFM) is based on the physical characteristics of light transmission in the atmosphere [29]. The model can be described as follows:

$$I^c(\mathrm{x})=J^c(\mathrm{x})\mathrm{t}(\mathrm{x})+A^c\left(1-t(\mathrm{x})\right),\ \ \mathrm{c}\in\{\mathrm{r},\ \mathrm{g},\ \mathrm{b}\} \tag{4}$$

where $I^c(\mathrm{x})$ is the observed intensity, $J^c(\mathrm{x})$ is the scene radiance, A^c is the ambient light, $t(\mathrm{x})$ is the transmission, and c is one of the RGB channels.

For each pixel x in an image, the DCP finds the minimum value among RGB channels in a local patch $\Omega(\mathrm{x})$ centered at x, which can be written as [30]:

$$J^{dark}(\mathrm{x})=\min_{y\in\Omega(\mathrm{x})}\left(\min_{c\in\{r,g,b\}}J^c(y)\right) \tag{5}$$

For an outdoor terrestrial sandstorm-free image, $J^{dark}(\mathrm{x})$ is often close to zero because at least one of the three color channels will typically have a low-intensity pixel in the local patch $\Omega(\mathrm{x})$ [30]. In sandstorm weather conditions, most blue light is scattered and absorbed, resulting in the blue light intensity decaying faster with increasing distance. We use the method in reference [31] to modify the DCP and obtain the blue channel, which can be written as:

$$J^{blue}(\mathrm{x})=\min\left(\min_{y\in\Omega(\mathrm{x})}\left(J^R(y)\right),\min_{y\in\Omega(\mathrm{x})}\left(J^G(y)\right),\min_{y\in\Omega(\mathrm{x})}\left(1-J^B(y)\right)\right)=0 \tag{6}$$

Tan [24] proposed that the brightest pixels are considered to be the most opaque in hazy images when the clouds are overcast. In this case, ambient light is the only source of illumination for the scene. Therefore, He et al. [30] proposed that the DCP of a hazy image is approximately similar to the haze density, so the DCP is used to detect the most opaque areas, thereby improving the estimation ability of ambient light. We select the deepest pixel from the camera because we assume that the sandstorm image degradation is related to the distance, which corresponds to the maximum value in the blue channel. We select the pixel x_0 in the degraded image as the ambient light, which corresponds to the brightest pixel in the blue channel and can be expressed as:

$$A^c=I(\mathrm{x}_0)=\left(A^R,\ A^G,1-A^B\right),\ I^{blue}(\mathrm{x}_0)\geq I^{blue}(\mathrm{x}) \tag{7}$$

Similar to the method proposed in [30], the brightest 0.1 percent pixels in the blue channel are extracted. Among these pixels, the pixel with the highest intensity in the degraded image is selected as the ambient light. However, this method of obtaining ambient light is not entirely suitable for sandstorm weather conditions. In sandstorm weather conditions, we first identify the 0.1 brightest pixels in the blue channel. Among these pixels, the pixel with the lower intensity of the blue component is selected as the ambient light value. The value we choose is the best result obtained from the experiments.

We can estimate the transmission based on the determined ambient light $A^c=\left(A^R,\ A^G,\ A^B\right)$, assuming that the transmission is constant in small local patches. The A^c on both sides of Eq. (4) are divided, and the minimum value is taken; combined with Eq. (6), we can find the transmission t(x), which can be written as:

$$\tilde{t}(\mathrm{x})=1-\min\left(\min_{y\in\Omega(\mathrm{x})}\frac{I^R(y)}{A^R},\min_{y\in\Omega(\mathrm{x})}\frac{I^G(y)}{A^G},\min_{y\in\Omega(\mathrm{x})}\frac{\left(1-I^B(y)\right)}{1-A^B}\right) \tag{8}$$

Finally, with ambient light and transmission, we can recover the scene radiance $J^c(\mathrm{x})$ according to (4), which can be written as:

$$J^c(\mathrm{x})=\frac{I^c(X)-A^c}{\max\left(t^c(\mathrm{x}),t_0\right)}+A^c \tag{9}$$

where a typical value for t_0 can be 0.1. Since the scene radiance is usually not as bright as the atmospheric light, the image after sandstorm removal looks dim. Therefore, we increased the exposure of $J^c(\mathrm{x})$ for display.

C. White balance

We use white balancing technology to eliminate color deviation to improve image quality, which can be roughly divided into light estimation and color correction. In some existing white balancing methods, a specific assumption is made to estimate the color of the light source, and then achieve color constancy by dividing each color channel by its corresponding normalized light source intensity. The gray-world algorithm [32] assumes that the average reflectance in the scene is achromatic. Therefore, by averaging each channel independently, the color distribution of the light source can be easily estimated. Max-RGB [33] assumes that the maximum response in each channel is caused by a white patch and therefore uses the maximum response of different color channels to estimate the color of the light source. In their 'shades-of-gray' method [34], Finlayson et al. first observed that max-RGB and gray-world are two instantiations of the Minkowski p-norm applied to the native pixels, with $p=\infty$ and $p = 1$, respectively, and proposed extending the process to arbitrary p values. The best results are obtained for $p = 6$.

In terms of color correction, through a comprehensive

This article has been accepted for publication in a future issue of this journal, but has not been fully edited. Content may change prior to final publication. Citation information: DOI 10.1109/ACCESS.2020.2985869, IEEE Access

comparison, we apply robust-AWB [35] to correct the color deviation of sandstorm images. This algorithm searches for gray pixels in images and compares the deviation of these gray pixels in YUV color space. Through iterative processing, we gradually corrected the color deviation.

D. Multi-scale fusion

In this work, we propose a sandstorm image enhancement method based on multi-scale fusion. Image fusion has shown utility in several applications, such as image compositing [36], multispectral video enhancement [37], defogging [38, 39] and HDR imaging [40]. Here, we propose a simple framework to enhance the visibility of sandstorm image scenes. We perform two different sandstorm-degraded image processing techniques on a single original image, which can enhance the image of sandstorm degradation.

1) Input to the fusion process

To obtain our first input, we use white balancing to process the original sandstorm-degraded image. This step aims to enhancing the image quality by eliminating color deviation. With increasing distance in a sandstorm environment, white balancing is obviously affected because the absorbed color is difficult to recover. The image after white balancing processing appears oversaturated, so we use gamma correction on the image. Gamma correction aims to correct the global contrast, which increases the difference between darker/lighter regions at the cost of a loss of details in the under/over-exposed regions.

To compensate for this loss, we derive a second input. We use multilayer decomposition to process the original sandstorm image, the blue channel to deal with the base layer to improve the contrast of the sandstorm-degraded image and white balancing technology to eliminate color deviation. The blue channel we proposed can restore short wavelength-dependent colors, which makes up for the difficulty of color recovery in the long distance of white balancing. The nonlinear mapping operation is used on the residual layer. The nonlinear mapping function can enhance the details of the image and make up for the loss of details caused by the first input due to gamma correction.

2) Weight of fusion process

After color correction and contrast enhancement, the output image still has the problems of blur and low visibility. To better improve the contrast and detail information of sandstorm-degraded images, we perform Laplacian contrast weight (W_L), saliency weight (W_S) and saturation weight (W_{sa}) processing on the two input images so that more pixels with high weight values can be represented in the final image.

W_L estimates the global contrast by calculating the absolute value of the Laplacian filter applied on each input luminance channel. However, for sandstorm-degraded images, applying only this weight is not enough to restore the contrast of sandstorm-degraded images, mainly because it cannot distinguish edges and flat areas well. To solve this problem, W_S is introduced.

W_S aims to emphasize the salient objects that lose their prominence in the sandstorm scene. We use the estimation method in [41] to measure the significance level. However, the saliency weight map tends to support the highlighted region. To overcome this limitation, we introduce another weight map based on the observation of the decrease in the saturation in the highlighted regions.

W_{sa} makes full use of the highly saturated region so that the fusion algorithm can adapt to the chromaticity information. The deviation between the K^{th} input luminance L_K and the R_K, G_K and B_K color channels can be calculated as follows:

$$W_{sa} = \sqrt{1/3\left[\left(R_K - L_K\right)^2 + \left(G_K - L_K\right)^2 + \left(B_K - L_K\right)^2\right]} \quad (10)$$

Next, we merge the three weight maps into one weight map. For each input k, an aggregated weight map W_K is obtained by summing the three W_L, W_S and W_{sa} weight maps. The K aggregated maps are then normalized on a pixel-per-pixel basis by dividing the weight of each pixel in each map by the sum of the weights of the same pixel over all maps. The normalized weight for each input can be calculated as:

$$\bar{W}_K = \frac{\left(W_K + \delta\right)}{\left(\sum_{K=1}^{K} W_K + K*\delta\right)} \quad (11)$$

where δ is a small regular term, which ensures that each input contributes to the output, and δ is set to 0.1.

3) Multi-scale fusion process

We use Laplacian pyramid multi-scale decomposition to achieve the multiresolution representation of the image. The basic idea of the Laplacian pyramid is to perform low-pass filtering and downsampling on the original image to obtain a rough scale approximate image that is the low-pass approximate image obtained by decomposition. After interpolation, filtering and calculating the difference between the approximate image and the original image, the decomposed bandpass component is obtained. The next level decomposition is carried out on the low-pass approximation image, and the multi-scale decomposition is completed iteratively. Using the Laplacian pyramid to decompose each input image into different scales, the enhanced image reconstruction process can be written as [42]:

$$R_L(\mathrm{x}) = \sum_{K=1}^{K} G_L\{\bar{W}_K(x)\} L_L\{I_K(x)\} \quad (12)$$

where l represents the number of layers in the pyramid, K represents the number of input images, and G_L and L_L represent the l^{th} layers of the Gaussian pyramid and the Laplacian pyramid.

As mentioned, the proposed algorithm framework is shown in Fig. 1. First, we address the initial image with white balancing and multilayer decomposition. White balancing is used to restore the fading features of the degraded image, and

This article has been accepted for publication in a future issue of this journal, but has not been fully edited. Content may change prior to final publication. Citation information: DOI 10.1109/ACCESS.2020.2985869, IEEE Access

multilayer decomposition is used to improve the details of the degraded image. Second, we carry out gamma correction for the image after the white balancing process, aiming to enhance the image contrast and to solving image oversaturation. Then, we use the blue channel to process the base layer and the nonlinear mapping operation to process the residual layer, which aims to enhance the contrast and detail information of the degraded image. Finally, we perform weight fusion processing to improve the edge information and clarity of the sandstorm-degraded image.

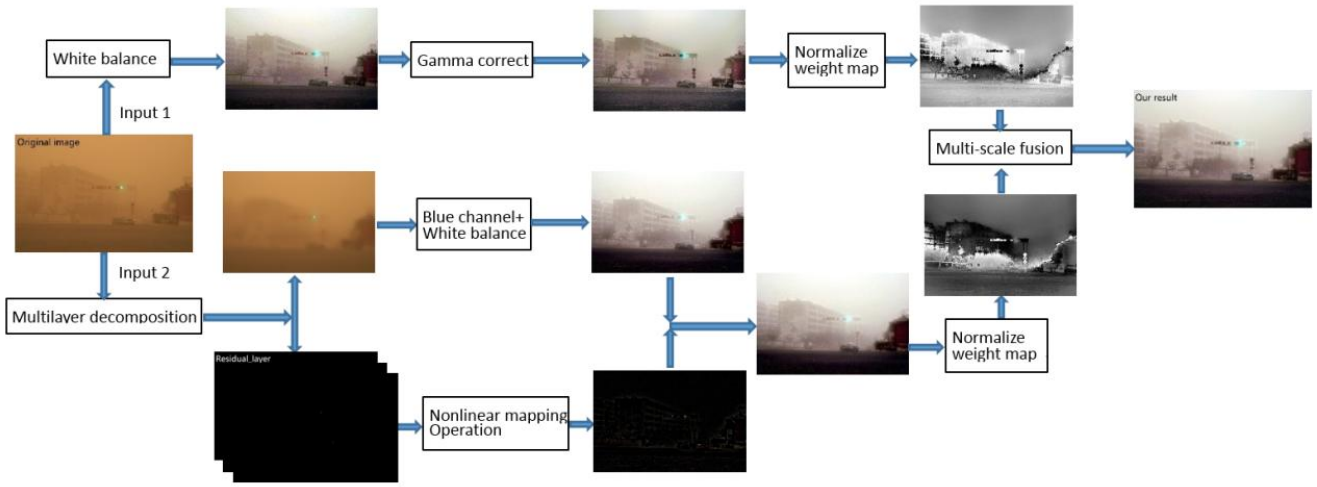

FIGURE 1. The framework of the proposed algorithm.

III. EXPERIMENTAL RESULTS

This section explores the subjective and objective evaluations to comprehensively compare the proposed method to the other methods. Other methods include those of He *et al*.[30], Alluhaidan [17], Li *et al*.[16], Fu *et al*.[19], Yang *et al*.[21] and Shi et al[3]. The evaluations are achieved using representative image databases, including Flickr [43] and Google Images [44], for a total sample set of 200 images. The experimental results in this paper consist of two major parts. Part A discusses the restoration results through subjective evaluation of images captured during sandstorm conditions. Part B uses the three well-known evaluation indicators adopted in [7, 8] to objectively evaluate the recovery results of the proposed method and other methods. To prove the effectiveness of the proposed method, all compared approaches were implemented in MATLAB 2018a on an Intel Core i5 3.20-GHz processor with 4 GB of RAM, running a Windows 7 operating system.

A. Subjective evaluation

As shown in Figs. 2–5, images restored via the methods of He *et al*.[30], Alluhaidan [17], Li *et al*.[16], Fu *et al*.[19], Yang *et al*.[21], Shi *et al*[3] and the proposed method were measured through visual evaluation of four sandstorm images titled "road," "driveway," "metropolis," and "edifice." During sandstorm weather conditions, captured images usually exhibit significant color deviation effects and inconsistent distributions of the RGB color channels due to most of the blue light being scattered and absorbed under sandstorm weather conditions.

As shown in Figs. 2(b)-(d)-5(b)-(d), the image processed by the algorithms in [30], [17], and [16] is still covered by sandstorm particles in the atmosphere, and there is a serious problem of color deviation, which does not achieve a satisfactory recovery effect. The reason for this phenomenon is that most of the blue light is scattered and absorbed in sandstorm weather conditions. Using the DCP or Retinex technology cannot accurately estimate the thickness of sandstorms. Compared with the methods in [30], [17] and [16], the proposed method can restore the clarity of the sandstorm-degraded image well, as shown in Figs. 2(h)-5(h). This is because we use blue channel technology to effectively recover short wavelength-dependent colors, which can accurately estimate the thickness of sandstorms.

As shown in Figs. 2(e)-(f)-5(e)-(f), the image processed by the algorithms in [19] and [21] effectively solves the color deviation and blur of sandstorms. However, the overall color of the image processed by [19] and [21] is cold, as shown in Figs. 2(e)-(f)-5(e)-(f). After processing [3], the image shows partial color fading and distortion. By observing the color of the wall and background in Fig. 4(g), we find that the algorithm has defects in image restoration of distant scenes. Compared with the methods in [3], [19] and [21], the proposed method can effectively solve the above problems and enhance the clarity in the image, as shown in Figs. 2(h)-5(h). In this study, 30 subjects were selected for the subjective evaluation of non-reference quality. Among them, 28 subjects considered the (h) images to be superior to the other images.

B. Objective evaluation

It is very difficult to objectively evaluate the recovered sandstorm-degraded image, because there is no real sandstorm-free image as a reference image to compare the restored image. The objective evaluation of recovery results can be divided into two categories: the reference method and

This article has been accepted for publication in a future issue of this journal, but has not been fully edited. Content may change prior to final publication. Citation information: DOI 10.1109/ACCESS.2020.2985869, IEEE Access

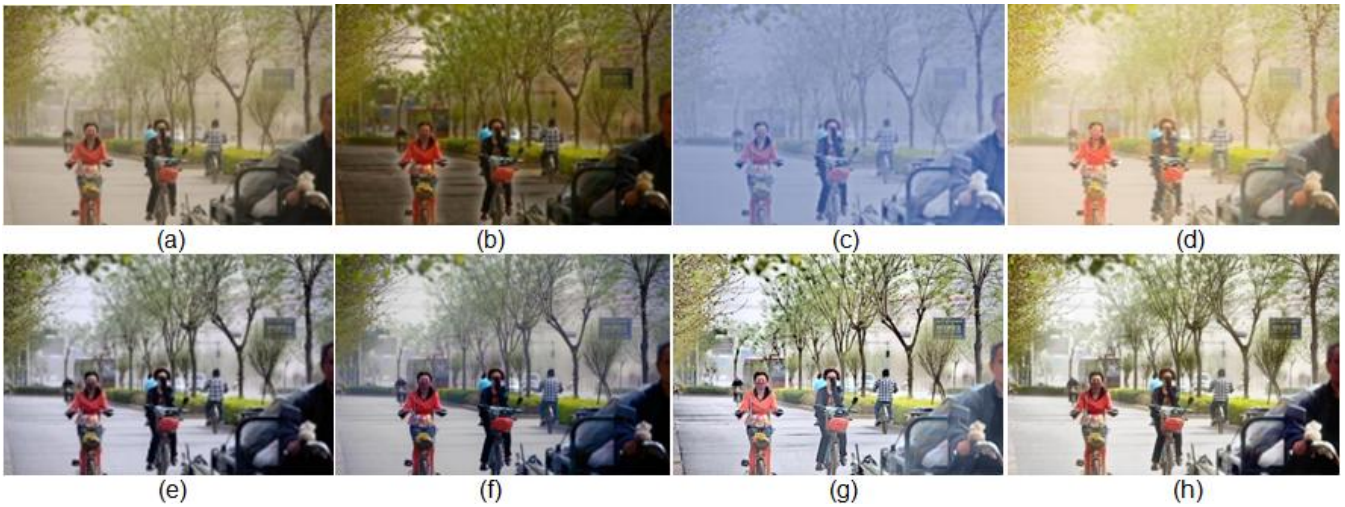

FIGURE 2. "Road" image. (a)Input sandstorm image. The remaining seven images are the restoration result generated by the methods of (b) He *et al*.[30], (c) Alluhaidan[17], (d) Li *et al*.[16], (e) Fu *et al*.[19], (f) Yang *et al*.[21], (g) Shi *et al*.[3], (h) the proposed method.

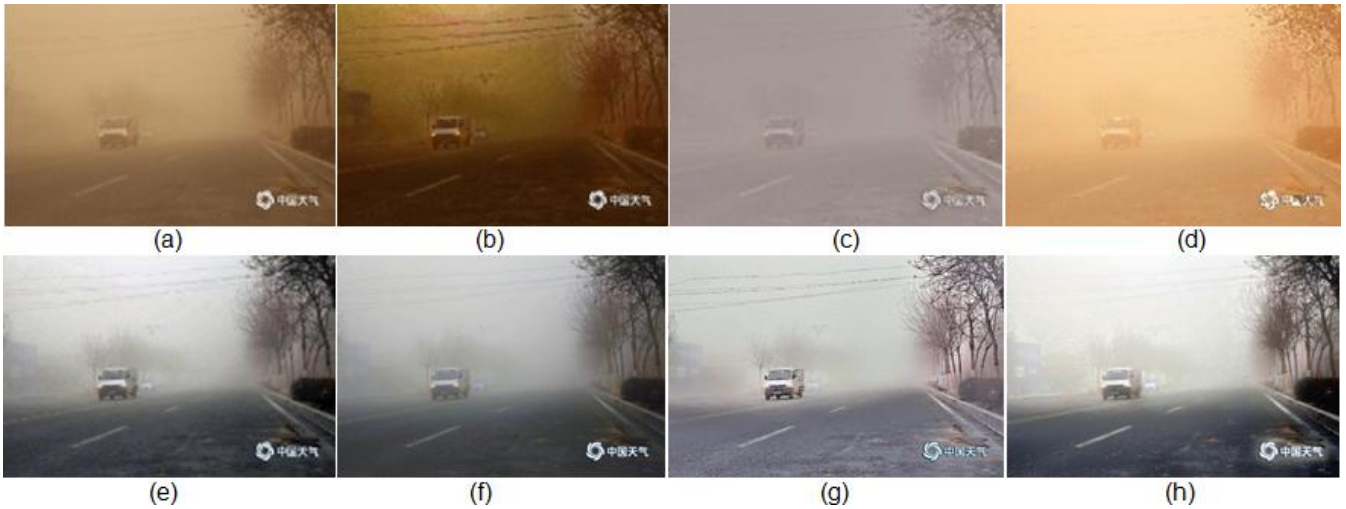

FIGURE 3. "Driveway" image. (a)Input sandstorm image. The remaining seven images are the restoration result generated by the methods of (b) He *et al*.[30], (c) Alluhaidan[17], (d) Li *et al*.[16], (e) Fu *et al*.[19], (f) Yang *et al*.[21], (g) Shi *et al*.[3], (h) the proposed method.

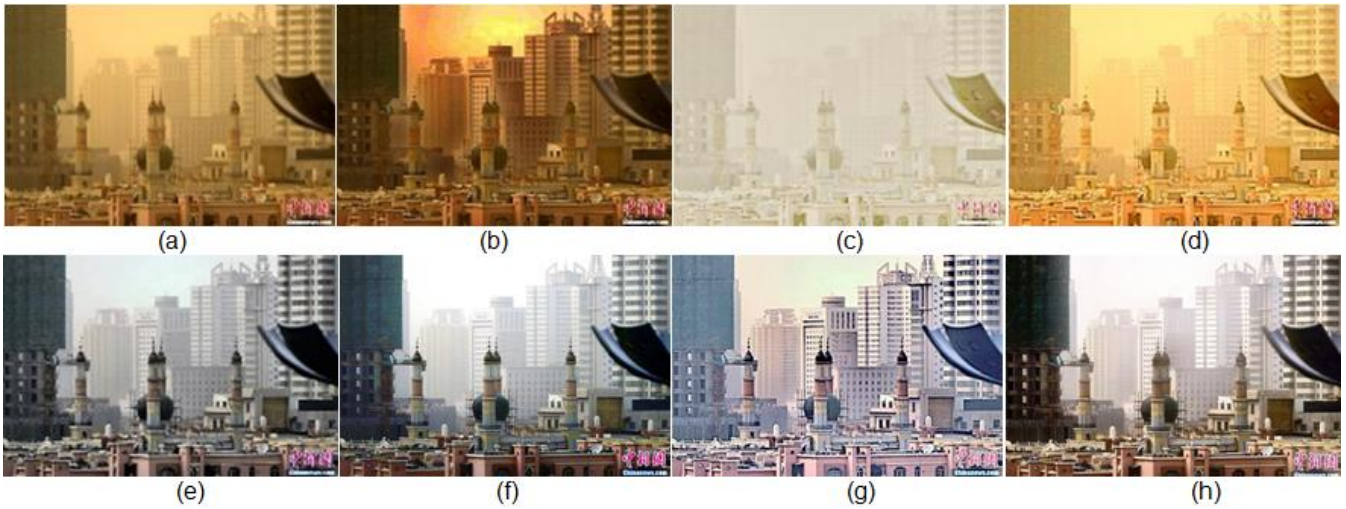

FIGURE 4. "Metropolis" image. (a)Input sandstorm image. The remaining seven images are the restoration result generated by the methods of (b) He *et al*.[30], (c) Alluhaidan[17], (d) Li *et al*.[16], (e) Fu *et al*.[19], (f) Yang *et al*.[21], (g) Shi *et al*.[3], (h) the proposed method.

This article has been accepted for publication in a future issue of this journal, but has not been fully edited. Content may change prior to final publication. Citation information: DOI 10.1109/ACCESS.2020.2985869, IEEE Access

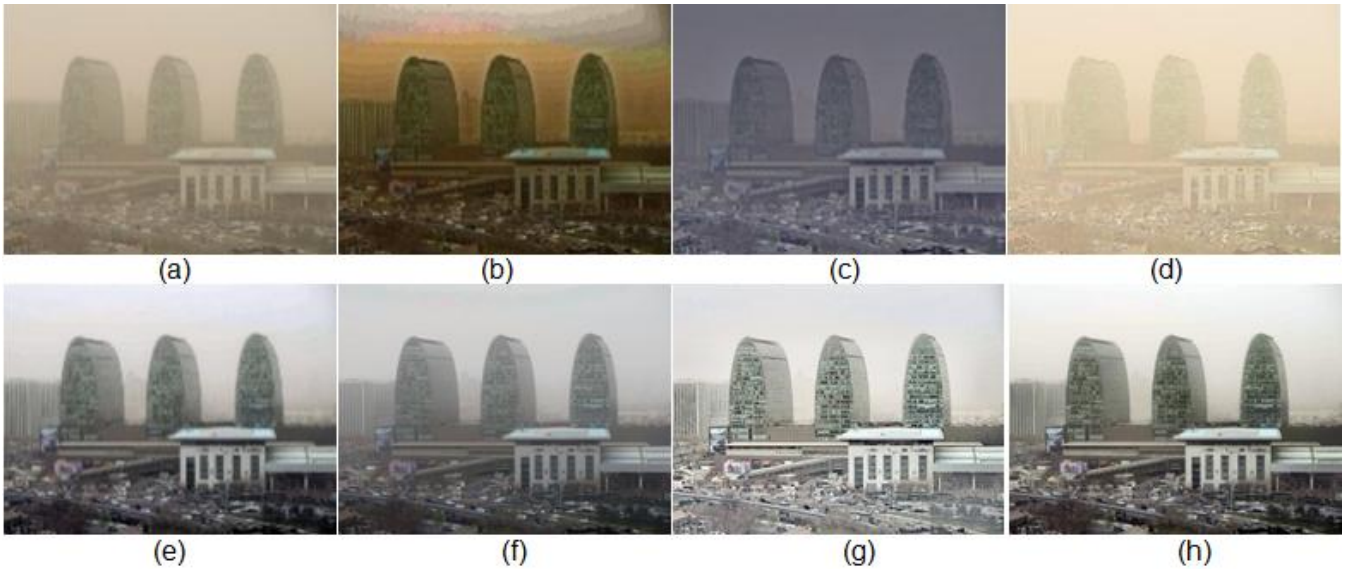

FIGURE 5. "Edifice" image. (a)Input sandstorm image. The remaining seven images are the restoration result generated by the methods of (b) He *et al*.[30], (c) Alluhaidan[17], (d) Li *et al*.[16], (e) Fu *et al*.[19], (f) Yang *et al*.[21], (g) Shi *et al*.[3], (h) the proposed method.

the non-reference method. Because we did not have a real sandstorm-free reference image, we used a non-reference method to analyze the restoration effect. We used three well-known objective evaluation metrics, e, $\bar{r}$ and σ [45], to evaluate the recovered sandstorm image. The e metric represents the ratio of the new visible edges in the sandstorm-free image:

$$e = \frac{n_r - n_0}{n_0} \tag{13}$$

where n_r is the number of visible edges in the recovered sandstorm image, and n_o is the number of visible edges in the original sandstorm image. The evaluation metric evaluates an edge restoration ability that is invisible in the original image but is visible in the restored image.

The $\bar{r}$ metric represents the quality of contrast restoration in sandstorm-free images. The expression can be written as follows:

$$\bar{r} = \exp\left[\frac{1}{V_r}\sum_{P_i \in \wp_r} \log\log(r_i)\right] \tag{14}$$

where $\bar{r}$ represents the gradient ratio between the restored sandstorm image and the original sandstorm image, and $\wp$ consists of the visible edges in the restored sandstorm image.

In addition, we also use the natural image quality evaluator (NIQE) [46] to evaluate the sandstorm-degraded images using the spatial domain natural scene statistics. Note that higher evaluation values e and $\bar{r}$ represent better recovery effects, while lower evaluation values NIQE represent better recovery effects.

Table 1-4 summarizes the results of image restoration under different concentrations of sandstorm weather conditions using the methods of He *et al*.[30], Alluhaidan [17], Li *et al*.[16], Fu *et al*.[19], Yang *et al*.[21], Shi et al[3] and the proposed method. In table 4, we adopted 200 images captured in varied sandstorm weather conditions with which to compare the results of each removal method. Observing the data, we find that the recovery effect obtained using the e, $\bar{r}$ and NIKE metrics is better than the methods of He *et al*.[30], Alluhaidan [17], Li *et al*.[16], Fu *et al*.[19] and Yang *et al*.[21]. Although the methods of Shi *et al*[3] is better than proposed method in $\bar{r}$, but our results are the best in terms of e, NIKE and computational complexity. At the same time, we measured the evaluation metrics ave, figure definition and shannon, and the results are better than other algorithms. Compared with other algorithms, our algorithm can effectively restore the reduced edge information in the image, as well as the detailed information and color features of the image. Therefore, through the objective comparison of the image restoration effect in different concentrations of sandstorm weather conditions, we can conclude that the effectiveness of the proposed algorithm is better than that of the other algorithms.

TABLE 1. SANDSTORM IMAGES OF FIGS. 2-5 RESTORED EVALUATION BASED ON THE ***e*** METRIC. A LARGER IS METRIC BETTER.

	Original	He et al.[30]	Alluhaidan.[17]	Li et al.[16]	Fu et al.[19]	Yang et al.[21]	Shi et al.[3]	Our method
Fig. 2	---	**0.960**	-0.377	-0.247	0.663	0.613	0.741	0.804
Fig. 3	---	2.698	-0.122	-0.225	2.590	1.511	3.411	**3.442**
Fig. 4	---	0.201	-0.678	-0.181	0.222	0.153	0.184	**0.292**
Fig. 5	---	1.700	1.394	-0.297	1.511	1.505	1.088	**1.701**
Average	---	1.415	0.054	-0.237	1.247	0.946	1.356	**1.560**

This article has been accepted for publication in a future issue of this journal, but has not been fully edited. Content may change prior to final publication. Citation information: DOI 10.1109/ACCESS.2020.2985869, IEEE Access

TABLE 2. SANDSTORM IMAGES OF FIGS. 2-5 RESTORED EVALUATION BASED ONTHE $\bar{\mathbf{r}}$ METRIC. A LARGER IS METRIC BETTER.

	Original	He et al.[30]	Alluhaidan.[17]	Li et al.[16]	Fu et al.[19]	Yang et al.[21]	Shi et al.[3]	Our method
Fig. 2	---	1.334	0.899	1.094	1.754	1.284	**3.780**	1.952
Fig. 3	---	2.145	0.993	1.198	2.535	1.486	**5.551**	2.798
Fig. 4	---	1.183	0.541	1.185	1.504	1.299	**2.981**	1.715
Fig. 5	---	2.251	1.931	1.025	2.854	1.974	**7.888**	3.306
Average	---	1.728	1.091	1.126	2.162	1.511	**5.050**	2.443

TABLE 3. SANDSTORM IMAGES OF FIGS. 2-5 RESTORED EVALUATION BASED ON THE **NIQE** METRIC. A SMALL IS METRIC BETTER.

	Original	He et al.[30]	Alluhaidan.[17]	Li et al.[16]	Fu et al.[19]	Yang et al.[21]	Shi et al.[3]	Our method
Fig. 2	2.414	2.749	3.234	2.625	2.519	2.531	2.614	**2.408**
Fig. 3	3.634	3.676	3.790	4.288	3.642	3.382	4.397	**3.192**
Fig. 4	3.743	3.691	4.518	4.169	3.639	3.518	4.191	**3.517**
Fig. 5	3.553	3.415	3.766	4.597	3.471	3.812	4.205	**3.262**
Average	3.337	3.383	3.827	3.920	3.318	3.311	3.852	**3.095**

TABLE 4. COMPARISON OF AVERAGE RESTORATION ACQUIRED BY THE ***e***, $\bar{\mathbf{r}}$ AND **NIQE** FOR 200 SANDSTORM IMAGES.

	Original	He et al.[30]	Alluhaidan.[17]	Li et al.[16]	Fu et al.[19]	Yang et al.[21]	Shi et al.[3]	Our method
e	--	1.415	0.039	-0.216	1.225	0.951	1.331	**1.621**
$\bar{\mathbf{r}}$	--	1.615	1.138	1.056	2.068	1.469	**5.021**	2.414
NIQE	4.102	3.961	4.345	4.410	3.855	3.761	4.343	**3.401**

C. Computational complexity

In this part, we will talk about the computational complexity of the proposed algorithm. As illustrated in Figures 1, the proposed algorithm includes multilayer decomposition, blue channel, enhancement, and multi-scale fusion. Therefore, the computational complexity of the proposed algorithm is the sum of computational complexities of these different processes. Let h and w represent the high and wide of the sandstorm images, c represents the number of layers processed, N is 0.1% of the total pixel, p is a constant. The computational complexity of each process in the proposed algorithm is shown in the following table. The entire algorithm is O ($h*w+2c^2$) as shown in Table 5.

TABLE 5. COMPLEXITY OF EACH PROCESS

Process	Complexity
multilayer decomposition	O(2c)
blue channel	O(h*w+N+3)
Multi-scale fusion	O($2c^2$)
Enhancement	O(p)
Proposed algorithm	O($h*w+2c^2$)

We also calculated the running time of the algorithm. Time complexity refers to the time used for algorithm implementation. For an image of size 900 × 600, the running times of the methods of He *et al*.[30], Alluhaidan[17], Li *et al*.[16], Fu *et al*.[19], Yang *et al*.[21], Shi et al[3] and the proposed method are shown in table 6. To better illustrate the effectiveness of the data, we test the time complexity of 20 images and then take the mean value, which is shown in table 6. By observing the data in table 6, we find that the time complexity of the proposed algorithm is lower than the time complexity of the methods of Shi *et al*[3] and Li *et al*.[16]. The proposed method requires more time than the methods of He *et al*.[30], Alluhaidan[17], Fu *et al*.[19] and Yang *et al*.[21], but our results are the best in terms of subjective and objective aspects.

TABLE 6. TIME COMPLEXITY OF EACH METHOD

Method	Time(s)	Average time(s)
He *et al*.[30]	4.17	4.01
Alluhaidan [17]	3.22	3.13
Li *et al*.[16]	41.87	38.33
Fu *et al*.[19]	3.48	3.244
Yang *et al*.[21]	3.23	3.101
Shi et al[3]	24.21	22.59
Our method	8.51	8.32

IV. DISCUSSION

This section discusses the difference between the proposed algorithm and image defogging algorithm, the proposed algorithm and the underwater image enhancement fusion algorithm respectively. In general , the defogging algorithm is an improved algorithm based on the DCP algorithm. We applied the defogging DCP algorithm to the sandstorm-degraded image, and there was serious color distortion and low contrast. Using the defogging DCP algorithm cannot accurately estimate the thickness of sandstorms. Therefore, the defogging DCP algorithm is not suitable for the enhancement of the sandstorm-degraded image, as shown in Figs. 2(b)-5(b). By testing the fusion algorithm of underwater image enhancement, we found that the fusion algorithm applied in the enhancement of sandstorm-degraded images has defects in the color restoration and contrast enhancement of the image. The color of restored images was darker, and there was still color distortion in the long-distance image, because the white balance algorithm can not solve the problem of color deviation in the long-distance image, and the gamma correction algorithm would cause the loss of detailed information. Therefore, we proposed a blue channel

algorithm that can enhance the contrast of images by recovering the short wave wavelength, and compensate for the fact that white balance cannot solve long-distance color deviation. We used a multilayer decomposition algorithm, and we selected the sigmoid function to enhance the image details and improve the image contrast. The subjective and objective experimental results show that our improved fusion algorithm was more suitable for enhancing sandstorm-degraded images.

V. CONCLUSION

In this paper, we propose a novel visibility restoration method based on a blue channel and fusion for recovering degraded images captured in sandstorm weather conditions. First, we use blue channel technology to enhance image contrast and white balancing technology to resolve the color distortion. Next, we use multilayer decomposition technology to enhance image details. Finally, we use multi-scale fusion technology to restore important faded features and edge information. The experimental results show that our proposed visibility restoration method based on a blue channel and fusion is better than other algorithms.

REFERENCES

[1] R. A. Priyadharshini and S. Aruna, "Visibility Enhancement Technique for Hazy Scenes," in *4th International Conference on Electrical Energy Systems, ICEES 2018, February 7, 2018 - February 9, 2018*, Chennai, India, 2018, pp. 540-545.

[2] Y. Wang, Y. Li, and T. Zhang, "Method to restore dust degraded images," *Huazhong Keji Daxue Xuebao (Ziran Kexue Ban)/Journal of Huazhong University of Science and Technology (Natural Science Edition)*, vol. 38, pp. 42-44+48, 2010.

[3] Z. H. Shi, Y. N. Feng, M. H. Zhao, E. H. Zhang, and L. F. He, "Let You See in Sand Dust Weather: A Method Based on Halo-Reduced Dark Channel Prior Dehazing for Sand-Dust Image Enhancement," *Ieee Access*, vol. 7, pp. 116722-116733, 2019.

[4] B.-H. Chen and S.-C. Huang, "Improved visibility of single hazy images captured in inclement weather conditions," in *15th IEEE International Symposium on Multimedia, ISM 2013, December 9, 2013 - December 11, 2013*, Anaheim, CA, United states, 2013, pp. 267-270.

[5] S. Y. Yu, H. Zhu, J. Wang, Z. F. Fu, S. Xue, and H. Shi, "Single sand-dust image restoration using information loss constraint," *Journal of Modern Optics*, vol. 63, pp. 2121-2130, 2016.

[6] Y.-T. Peng and P. C. Cosman, "Single image restoration using scene ambient light differential," in *23rd IEEE International Conference on Image Processing, ICIP 2016, September 25, 2016 - September 28, 2016*, Phoenix, AZ, United states, 2016, pp. 1953-1957.

[7] Y. T. Peng, K. M. Cao, and P. C. Cosman, "Generalization of the Dark Channel Prior for Single Image Restoration," *Ieee Transactions on Image Processing*, vol. 27, pp. 2856-2868, Jun 2018.

[8] S. C. Huang, J. H. Ye, and B. H. Chen, "An Advanced Single-Image Visibility Restoration Algorithm for Real-World Hazy Scenes," *Ieee Transactions on Industrial Electronics*, vol. 62, pp. 2962-2972, May 2015.

[9] S.-C. Huang, B.-H. Chen, and Y.-J. Cheng, "An efficient visibility enhancement algorithm for road scenes captured by intelligent transportation systems," *IEEE Transactions on Intelligent Transportation Systems*, vol. 15, pp. 2321-2332, 2014.

[10] S. C. Huang, B. H. Chen, and W. J. Wang, "Visibility Restoration of Single Hazy Images Captured in Real-World Weather Conditions," *Ieee Transactions on Circuits and Systems for Video Technology*, vol. 24, pp. 1814-1824, Oct 2014.

[11] H. Dong and X. Wang, "Methods of restoring a weather degradation image based on physical model and their application," *in Proceedings - International Conference on Electrical and Control Engineering*, ICECE 2010, 2010, pp. 5323-5326.

[12] W. Jin-Song, A. Chao, and Y. Peng, "Method and application of image clearness in bad weather," *in 2010 International Conference on Communications and Mobile Computing*, CMC 2010, April 12, 2010 - April 14, 2010, Shenzhen, China, 2010, pp. 40-44.

[13] Y. Y. Schechner and Y. Averbuch, "Regularized image recovery in scattering media," *IEEE Transactions on Pattern Analysis and Machine Intelligence*, vol. 29, pp. 1655-1660, 2007.

[14] S. G. Narasimhan and S. K. Nayar, "Chromatic framework for vision in bad weather," in *CVPR '2000: IEEE Conference on Computer Vision and Pattern Recognition, June 13, 2000 - June 15, 2000*, Hilton Head Island, SC, USA, 2000, pp. 598-605.

[15] S. K. Nayar and S. G. Narasimhan, "Vision in bad weather," in *Proceedings of the 1999 7th IEEE International Conference on Computer Vision (ICCV'99), September 20, 1999 - September 27, 1999*, Kerkyra, Greece, 1999, pp. 820-827.

[16] M. Li, J. Liu, W. Yang, X. Sun, and Z. Guo, "Structure-Revealing Low-Light Image Enhancement Via Robust Retinex Model," *IEEE Transactions on Image Processing*, vol. 27, pp. 2828-2841, 2018.

[17] M. Alluhaidan, "Retinex-Based Framework for Visibility Enhancement During Inclement Weather with Tracking and EstimatingDistance of Vehicles," 2019IEEEJordan International Joint Conference in Electrical Engineering and information Technology(JEEIT), pp. 250-255, 2019.

[18] T. Yan, L. J. Wang, J. X. Wang, "Method to Enhance Degraded Image in Dust Environment," *Journal of software*, vol. 9, pp. 2672-2677, Oct 2014.

[19] X. Fu, Y. Huang, D. Zeng, X.-P. Zhang, and X. Ding, "A fusion-based enhancing approach for single sandstorm image," in *2014 16th IEEE International Workshop on Multimedia Signal Processing, MMSP 2014, September 22, 2014 - September 24, 2014*, Jakarta, Indonesia, 2014.

[20] X. Wang, Y. Ju, and T. Gao, "Enhancement techniques for degraded traffic video images under sandstorms based on fractional differential," *Qinghua Daxue Xuebao/Journal of Tsinghua University*, vol. 52, pp. 61-64+68, 2012.

[21] Y. Yang, C. Zhang, L. Liu, G. Chen, and H. Yue, "Visibility restoration of single image captured in dust and haze weather conditions," *Multidimensional Systems and Signal Processing* 2019.

[22] M. Alruwaili and L. Gupta, "A statistical adaptive algorithm for dust image enhancement and restoration," *in IEEE International Conference on Electro/Information Technology*,EIT 2015, May 21, 2015 - May 23, 2015, Dekalb, IL, United states, 2015, pp. 286-289.

[23] J. Wang, Y. Pang, Y. He, and C. Liu, "Enhancement for dust-sand storm images,"*in 22nd International Conference on MultiMedia Modeling*,MMM 2016, January 4, 2016 - January 6, 2016, Miami, FL, United states, 2016, pp. 842-849.

[24] R. T. Tan, "Visibility in bad weather from a single image," in *26th IEEE Conference on Computer Vision and Pattern Recognition, CVPR, June 23, 2008 - June 28, 2008*, Anchorage, AK, United states, 2008.

[25] K. He, J. Sun, and X. Tang, " Guided image filtering," *Ieee Trans. Pattern Anal. Mach. Intell*, vol. 35, pp. 1397–1409, Jun. 2013.

[26] H. Talebi and P. Milanfar, "Fast Multilayer Laplacian Enhancement," *Ieee Transactions on Computational Imaging*, vol. 2, pp. 496-509, Dec 2016.

[27] H. Pan, R. Tian, C. Liu, and C. Gong, "A Sand-Dust Degraded Image Enhancement Algorithm Based on Color Correction and Information Loss Constraints," *Jisuanji Fuzhu Sheji Yu Tuxingxue Xuebao/Journal of Computer-Aided Design and Computer Graphics*, vol. 30, pp. 992-999, 2018.

[28] Z. Ning, S. Mao, and L. Mei, "Visibility restoration algorithm of dust-degraded images," *Journal of Image & Graphics*, 2016.

[29] R. Fattal, " Single image dehazing, " *ACM Trans. Graph*, vol. 27, pp. 72-72, Aug 2008.

[30] K. M. He, J. Sun, and X. O. Tang, "Single Image Haze Removal Using Dark Channel Prior," *Ieee Transactions on Pattern Analysis and Machine Intelligence*, vol. 33, pp. 2341-2353, Dec 2011.

[31] A. Galdran, D. Pardo, A. Picon, and A. Alvarez-Gila, "Automatic Red-Channel underwater image restoration," *Journal of Visual Communication and Image Representation*, vol. 26, pp. 132-145, Jan 2015.

[32] G. Buchsbaum, "A spatial processor model for object colour perception," Journal of the Franklin Institute, vol. 310, pp. 1-26,1980.

[33] Land and E. H., "The Retinex Theory of Color Vision," Scientific American, vol. 237, pp. 108-128.

[34] G. D. Finlayson and E. Trezzi, "Shades of gray and colour constancy," in Final Program and Proceedings of the IS and T and SID - 12th Color Imaging Conference: Color Science and Engineering: Systems, Technologies, Applications, November 9, 2004 - November 12, 2004, Scottsdale, AZ, United states, 2004, pp. 37-41.

[35] J. Y. Huo, Y. L. Chang, J. Wang, and X. X. Wei, "Robust automatic white balance algorithm using gray color points in images," Ieee Transactions on Consumer Electronics, vol. 52, pp. 541-546, May 2006.

[36] M. Grundland, R. Vohra, G. P. Williams, and N. A. Dodgson, "Cross Dissolve Without Cross Fade: Preserving Contrast, Color and Salience in Image Compositing," Computer Graphics Forum, vol. 25, pp. 577-586.

[37] E. P. Bennett, J. L. Mason, and L. McMillan, " Multi-spectral bilat-eral video fusion," IEEE Trans. Image Process , vol. 16, pp. 1185–1194, May 2007.

[38] C. O. Ancuti and C. Ancuti, "Single image dehazing by multi-scale fusion," IEEE Transactions on Image Processing, vol. 22, pp. 3271-3282, 2013.

[39] C. Ancuti and P. Bekaert, "Effective Single Image Dehazing by Fusion," in Image Processing (ICIP), 2010 17th IEEE International Conference on, 2010.

[40] T. Mertens, J. Kautz, and F. Van Reeth, "Exposure fusion: A simple and practical alternative to high dynamic range photography," Computer Graphics Forum, vol. 28, pp. 161-171, 2009.

[41] C. Ancuti, C. O. Ancuti, T. Haber, and P. Bekaert, "Enhancing Underwater Images and Videos by Fusion," in 2012 IEEE Conference on Computer Vision and Pattern Recognition, 2012.

[42] P. J. Burt and E. H. Adelson, "LAPACIAN PYRAMID AS A COMPACT IMAGE CODE," IEEE Transactions on Communications, vol. COM-31, pp. 532-540, 1983.

[43] Explore—Flickr. [Online]. Available: http://www.flickr.com/

[44] Google Images. [Online]. Available: http://images.google.com/

[45] N. Hautiere, J. P. Tarel, D. Aubert, and E. Dumont, "Blind contrast enhancement assessment by gradient ratioing at visible edges.(Report)," vol. 27, pp. 87-95, 2011.

[46] A. Mittal, R. Soundararajan, and A. C. Bovik, " Making a 'completelyblind' image quality analyzer,"IEEE Signal Process. Lett, vol. 20, pp.209-212, Mar. 2013.

YAQIAO CHENG received the B.S. degree from the Department of Information Science and Engineering, Xinjiang University, Urumqi, China, in 2017. He is currently pursuing the master's degree from the School of Information Science and Engineering, Xinjiang University, China. His research direction is the clarity of video and images in sandstorm conditions.

ZHENHONG JIA received the B.S. degree from Beijing Normal University, Beijing, China, in 1985, and the M.S. and Ph.D. degrees from Shanghai Jiao Tong University, Shanghai, China, in 1987 and 1995. Currently, he is a professor at the Autonomous University Key Laboratory of signal and information processing laboratory, Xinjiang University, China. His research interests include digital image processing, Photoelectric information detection and sensor.

HUICHENG LAI received the B.E. and M.S. Degrees from Xinjiang university in 1986 and 1990, respectively. He is currently a Professor with Xinjiang University, China. His current research interests include image processing, image recognition, image enhancement, image restoration and communications technology. Mailing addresses: 666 Shengli Road, Urumqi, Xinjiang University, China.

JIE YANG received his Ph.D. degree from the Department of Computer Science, Hamburg University, Germany, in 1994. Currently, he is a professor at the Institute of Image Processing and Pattern Recognition, Shanghai Jiao Tong University, China. His major research interests include object detection and recognition, data fusion and data mining, and medical image processing.

NIKOLA K. KASABOV (M'93–SM'98–F'10) received the M.S. degree in computing and electrical engineering and the Ph.D. degree in mathematical sciences from the Technical University of Sofia, Sofia, Bulgaria, in 1971 and 1975, respectively. He is currently the Director and the Founder of the Knowledge Engineering and Discovery Research Institute and a Professor of knowledge engineering with the School of Computing and Mathematical Sciences, Auckland University of Technology, Auckland, New Zealand. His major research interests include information science, computational intelligence, neural networks, bioinformatics, and neuroinformatics.